Title

False Negatives for Remote Life Detection on Ocean-Bearing Planets: Lessons from the Early Earth

Journal

Astrobiology, 17(4)

ISSN

1531-1074

Authors

Reinhard, Christopher T
Olson, Stephanie L
Schwieterman, Edward W
et al.

Publication Date

2017-04-01

DOI

10.1089/ast.2016.1598

Peer reviewed

ASTROBIOLOGY
Volume 17, Number 4, 2017
Mary Ann Liebert, Inc.
DOI: 10.1089/ast.2016.1598

Rapid Communication

False Negatives for Remote Life Detection on Ocean-Bearing Planets: Lessons from the Early Earth

Christopher T. Reinhard,[1,2] Stephanie L. Olson,[1,3] Edward W. Schwieterman,[1,3,4,5] and Timothy W. Lyons[1,3]

Abstract

Ocean-atmosphere chemistry on Earth has undergone dramatic evolutionary changes throughout its long history, with potentially significant ramifications for the emergence and long-term stability of atmospheric biosignatures. Though a great deal of work has centered on refining our understanding of *false positives* for remote life detection, much less attention has been paid to the possibility of *false negatives*, that is, cryptic biospheres that are widespread and active on a planet's surface but are ultimately undetectable or difficult to detect in the composition of a planet's atmosphere. Here, we summarize recent developments from geochemical proxy records and Earth system models that provide insight into the long-term evolution of the most readily detectable potential biosignature gases on Earth—oxygen (O_2), ozone (O_3), and methane (CH_4). We suggest that the canonical O_2-CH_4 disequilibrium biosignature would perhaps have been challenging to detect remotely during Earth's $\sim$4.5-billion-year history and that in general atmospheric O_2/O_3 levels have been a poor proxy for the presence of Earth's biosphere for all but the last $\sim$500 million years. We further suggest that detecting atmospheric CH_4 would have been problematic for most of the last $\sim$2.5 billion years of Earth's history. More broadly, we stress that internal oceanic recycling of biosignature gases will often render surface biospheres on ocean-bearing silicate worlds cryptic, with the implication that the planets most conducive to the development and maintenance of a pervasive biosphere will often be challenging to characterize via conventional atmospheric biosignatures. Key Words: Biosignatures—Oxygen—Methane—Ozone—Exoplanets—Planetary habitability. Astrobiology 17, 287–297.

1. Introduction

In the two decades since the first radial velocity surveys detected distant planets orbiting Sun-like stars (Mayor and Queloz, 1995), the burgeoning field of exoplanet research has yielded an astonishing number and diversity of extrasolar worlds. At the time of this writing, there are 2331 confirmed exoplanets, with an additional 2365 candidate planets in the Kepler field of view (Akeson *et al.,* 2013), many of which will likely be confirmed as additional exoplanets. The size, orbital parameters, and composition of these planets are staggering in their diversity (*e.g.,* Pierrehumbert, 2013), and the continued discovery and characterization of these worlds may ultimately have the potential to yield our first evidence for life beyond Earth.

Despite the anticipation that detection and analysis of exoplanetary atmospheres would be difficult or impossible to perform routinely, over three dozen exoplanetary atmospheres have been observed to date (Seager and Deming, 2011; Seager, 2013). The next generation of space telescopes, including the James Webb Space Telescope (JWST) and Transiting Exoplanet Survey Satellite (TESS), are expected to detect and/or characterize a number of transiting exoplanets in unprecedented detail (see, for example, Gardner *et al.,* 2006; Deming *et al.,* 2009; Cowan *et al.,* 2015). Large space-based telescope missions currently in their science definition phase would possess the capability to directly image terrestrial exoplanets at UV to near-IR wavelengths (*e.g.,* Dalcanton *et al.,* 2015; Mennesson *et al.,* 2016), while future ground-based observatories will also be able to spectrally characterize

[1]NASA Astrobiology Institute.
[2]School of Earth and Atmospheric Sciences, Georgia Institute of Technology, Atlanta, Georgia.
[3]Department of Earth Sciences, University of California, Riverside, California.
[4]NASA Postdoctoral Program, Universities Space Research Association, Columbia, Maryland.
[5]Blue Marble Space Institute of Science, Seattle, Washington.

the atmospheres of small planets around the very nearest stars (*e.g.,* Snellen *et al.,* 2013, 2015). Indeed, for the foreseeable future our only accessible method for detecting life or even fully characterizing habitability beyond Earth will likely be deciphering the chemistry of exoplanetary atmospheres (Meadows and Seager, 2010; Seager, 2014).

The prospect of remotely analyzing the composition of potentially habitable exoplanetary surfaces and atmospheres provides strong impetus for the development of biosignatures that can be used to diagnose the presence and scope of a surface biosphere. The most prominent of these approaches emphasize the potential of a planet's biosphere to reshape atmospheric chemistry and in particular to drive chemical disequilibrium via large production fluxes of incompatible volatile species (Lovelock, 1965; Hitchcock and Lovelock, 1967; Sagan *et al.,* 1993; Kaltenegger *et al.,* 2007; Meadows and Seager, 2010; Seager *et al.,* 2013a; Krissanson-Totton *et al.,* 2016). The most frequently cited example of this concept is the coexistence of molecular oxygen (O_2) and methane (CH_4) in the modern Earth's atmosphere at abundances that are many orders of magnitude out of thermodynamic equilibrium (*e.g.,* Hitchcock and Lovelock, 1967), but this concept can be functionally extended to include, for example, the coexistence of N_2, O_2, and H_2O in Earth's modern ocean-atmosphere system at levels strongly out of thermodynamic equilibrium with aqueous H^+ and NO_3^- (Krissanson-Totton *et al.,* 2016).

Significant effort has been expended to understand abiotic mechanisms for generating the most prominent among the possible atmospheric biosignatures, particularly false-positive signatures based on oxygen (O_2) and ozone (O_3). A number of ''pathological'' high-O_2 scenarios are now known, including those that involve (1) hydrogen escape from atmospheres depleted in noncondensing gases (Wordsworth and Pierrehumbert, 2014), (2) CO_2 photolysis in very dry atmospheres (Gao *et al.,* 2015), (3) atmospheres undergoing runaway water loss (Luger and Barnes, 2015), and (4) modest photochemical production of O_2/O_3 from CO_2 photolysis on planets around certain types of host star (Segura *et al.,* 2007; Domagal-Goldman *et al.,* 2014; Harman *et al.,* 2015). Although the diversity of mechanisms for generating high O_2/O_3 levels on lifeless worlds sounds an important cautionary note in the search for compelling biosignatures, these studies also identified a suite of contextual tools that can be used to diagnose high-O_2 false positives under many circumstances (Domagal-Goldman *et al.,* 2014; Harman *et al.,* 2015; Schwieterman *et al.,* 2015, 2016).

Biosignatures in reducing planetary atmospheres have been less explored (Domagal-Goldman *et al.,* 2011; Seager *et al.,* 2013b). This gap is important, as Earth's atmosphere has been relatively reducing—but not H_2-dominated—for most of its history (*e.g.,* Lyons *et al.,* 2014), and it is currently unknown whether the evolution of water-splitting (oxygenic) photosynthesis should be expected to be a common phenomenon beyond our solar system. Indeed, even if energetic benefits make the evolution of oxygenic photosynthesis probable on habitable planets, this alone may not be enough. For example, Earth's atmosphere may have remained strongly reducing for 500 million years or more after the emergence of biological O_2 production (Catling and Claire, 2005; Planavsky *et al.,* 2014a). As a result, there is little *a priori* reason to expect that most life-bearing extrasolar worlds will be characterized by atmospheres rich in biogenic O_2, particularly given our intrinsically brief timescale of observation relative to the potential timescales of planetary oxygenation.

An additional issue that has not been fully explored is that atmospheric chemistry on ocean-bearing planets can be strongly decoupled from overall surface metabolic fluxes due to internal microbial recycling within a planet's oceanic biosphere. For example, some of the largest input/output fluxes in Earth's modern biological CH_4 cycle occur via the microbial production and oxidation of CH_4 in deep marine sediments (Reeburgh, 2007), and this cycle is entirely decoupled from Earth's atmospheric CH_4 inventory. Indeed, most of this cycling occurs through anaerobic processes in the ocean (Valentine, 2011) and can occur through a number of common electron acceptors that will not necessarily be in equilibrium with corresponding atmospheric gases (Martens and Berner, 1977; Hoehler *et al.,* 1994; Regnier *et al.,* 2011; Sivan *et al.,* 2011; Deutzmann *et al.,* 2014; Riedinger *et al.,* 2014). As a result, internal recycling by ocean biospheres may inhibit the development or erode the stability of atmospheric biosignatures despite large production rates of biosignature gases. Such oceanic filtering of atmospheric biosignatures could in principle occur on a wide range of ocean-bearing silicate planets and in many cases will be an important process even on reducing planetary surfaces.

A second example is provided by the possibility of a cryptic oxygenic biosphere. In Earth's oceans, slow air-sea exchange of O_2 relative to high local rates of biological production in the surface waters can result in large regions of the surface ocean that are strongly out of equilibrium with atmospheric pO_2, by as much as a factor of $\sim 10^4$ (Kasting, 1991; Olson *et al.,* 2013; Reinhard *et al.,* 2013a, 2016). Thus, despite vigorous biological O_2 production in the shallowest oceanic environments, a planetary atmosphere can remain pervasively reducing as a result of either low globally integrated surface fluxes or elevated atmospheric sinks (or some combination). Such planets may be capable of accumulating significant quantities of reduced biosignature gases but will be false negatives for the presence of oxygenic photosynthesis and will have limited capacity for preservation and detection of associated oxidized biosignatures gases (*e.g.,* O_3, N_2O).

As a proof on concept, we briefly summarize the remote detectability of O_2/O_3, CH_4, and the O_2-CH_4 disequilibrium throughout Earth's history. Our analysis suggests that the O_2-CH_4 disequilibrium approach would have failed for most of Earth's history, particularly for observations at low to moderately high spectral resolving power ($R \leq 10{,}000$). In addition, it is possible that O_2/O_3 may only have been applicable as a potential biosignature during the last $\sim 10\%$ of Earth's lifetime. As a result, most of our planet's history may have been characterized by either high abundances of a single biogenic gas that can also have significant abiotic sources (*e.g.,* CH_4) or by a cryptic biosphere that was widespread and active at the surface but remained ultimately unrepresented in the detectable composition of Earth's atmosphere. Finally, we argue that cryptic biospheres may be a particularly acute problem on ocean-bearing planets, with the implication that many of the most favorable planetary hosts for surface biospheres will also have high potential for attenuation of atmospheric biosignatures.

2. Evolution of Atmospheric O_2/O_3 during Earth's History

The most compelling quantitative insights into atmospheric O_2 abundance during Archean time (~3.8–2.5 Ga) come from the observation of large non-mass-dependent sulfur isotope anomalies in sulfide and sulfate minerals deposited in coeval marine sediments (Farquhar *et al.,* 2000, 2001; reviewed in Johnston, 2011). When interpreted in the context of photochemical models (Pavlov and Kasting, 2002; Ono *et al.,* 2003; Zahnle *et al.,* 2006; Ueno *et al.,* 2009), the presence of these isotopic anomalies implies a ground-level atmospheric pO_2 value that was below 10^{-5} times the present atmospheric level (PAL) and more likely below $\sim 10^{-7}$ PAL (*e.g.,* Claire *et al.,* 2006; Zahnle *et al.,* 2006). Though there is some evidence for transient periods of elevated pO_2 during the Archean (Anbar *et al.,* 2007; Reinhard *et al.,* 2009; Kendall *et al.,* 2015), these deviations are poorly understood from a quantitative standpoint, and the overall background state during Archean time appears to have been one of exceptionally low atmospheric O_2. The sulfur isotope anomalies fingerprinting extremely low atmospheric O_2 disappear relatively rapidly during the Great Oxidation Event (GOE) of the early Paleoproterozoic (Holland, 2002; Luo *et al.,* 2016) and are not seen again in typical marine sedimentary rocks for the remainder of Earth's history (Fig. 1).

Unfortunately, the rather extreme sensitivity of the sulfur isotope system to very low levels of O_2 in the atmosphere makes it unfeasible to quantitatively diagnose changes in atmospheric composition once pO_2 increased above ~1–2 ppmv during the GOE. As a result, atmospheric O_2 levels for most of the subsequent ~2.5 billion years of Earth's history are rather poorly constrained. There is some evidence from the geochemical record for a transient, though protracted, rise in atmospheric pO_2 during the Paleoproterozoic (Schröder *et al.,* 2008; Planavsky *et al.,* 2012; Partin *et al.,* 2013; Canfield *et al.,* 2015), perhaps to levels that would have rivaled those of the modern Earth (Fig. 1). However, this evidence remains somewhat fragmentary at present and is difficult to evaluate quantitatively.

Nevertheless, a number of geochemical records point to low atmospheric pO_2 for extended periods of Earth's history well after the GOE. For example, the apparent loss of Fe (and in some cases Mn) as dissolved reduced species from paleosols (ancient weathering profiles) during some periods of the Proterozoic (Holland, 1984) and the general lack of significant chromium (Cr) isotope fractionation in marine

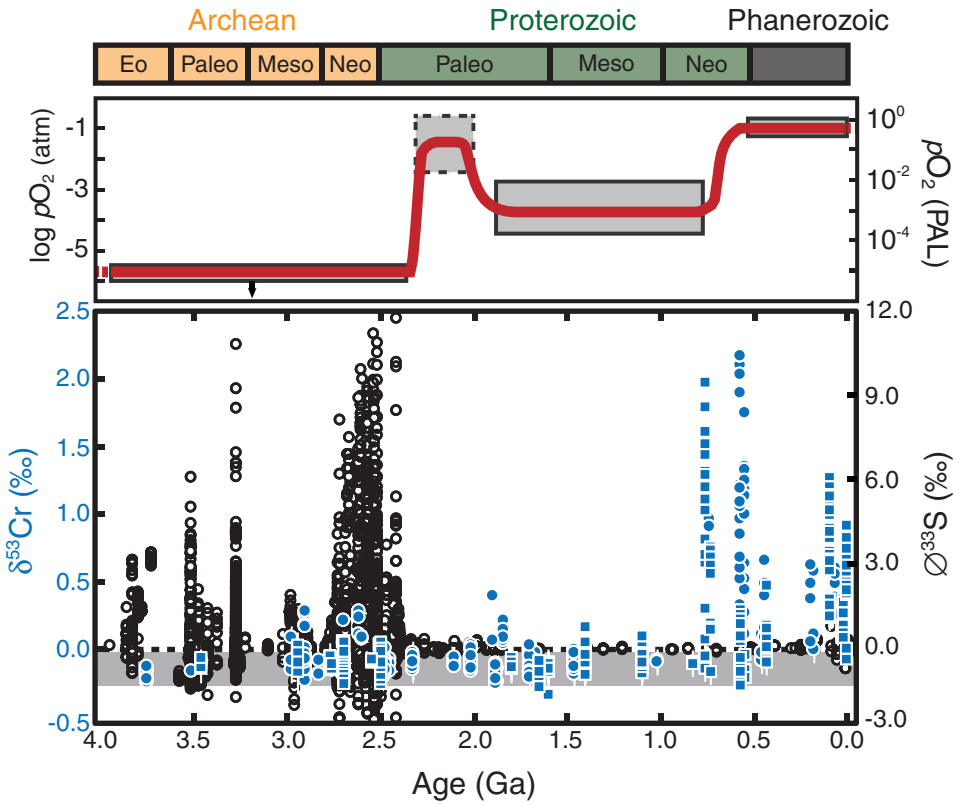

FIG. 1. Atmospheric O_2 on Earth through time (upper) and select geochemical proxies for atmospheric pO_2 (lower). In the upper panel, shaded boxes show approximate ranges based on geochemical proxy reconstructions, while the red curve shows one possible trajectory through time. In the lower panel, open circles show the magnitude of non-mass-dependent sulfur isotope (NMD-S) anomalies, shown as $\Delta^{33}S$ (see Johnston, 2011) and compiled as in Reinhard *et al.* (2013b). Filled blue symbols show chromium (Cr) isotope fractionations from iron-rich and siliciclastic marine sedimentary rocks throughout Earth's history (Cole *et al.,* 2016). We show these particular proxies in order to optically emphasize the three major periods of Earth's history discussed here: the Archean (~3.8–2.5 Ga), the Proterozoic (~2.5–0.5 Ga), and the Phanerozoic (~500 Ma to the present). See Lyons *et al.* (2014) for a more in-depth recent discussion of atmospheric O_2 proxies and evolution through time.

Table 1. Atmospheric pO_2 and pCH_4 Values for Different Geological Epochs Used in Our Spectral Calculations

Age		pO_2 *(PAL)*		pCH_4 *(ppmv)*	
Stratigraphic	*Ma*	*Low*	*High*	*Low*	*High*
Archean	3800–2500	—	10^{-5}	10^{2}	10^{3}
Lomagundi	2200–2000	10^{-2}	2.0	0.7	6
mid-Proterozoic	1800–800	$10^{-3.3}$	10^{-2}	1	20
Phanerozoic	543–0	0.25	1.4	0.7	6

Values for pO_2 are approximated according to Rye and Holland (1998), Pavlov and Kasting (2002), Bergman *et al.* (2004), Glasspool and Scott (2010), Crowe *et al.* (2013), Lyons *et al.* (2014), Planavsky *et al.* (2014b), and Tang *et al.* (2016). Values for pCH_4 are approximated according to Pavlov *et al.* (2000, 2003), Claire *et al.* (2006), Zahnle *et al.* (2006), Catling *et al.* (2007), Bartdorff *et al.* (2008), and Olson *et al.* (2016).

sediments (Planavsky *et al.,* 2014b; Cole *et al.,* 2016) are both consistent with very low atmospheric pO_2 between $\sim$1.8 and 0.8 Ga (Fig. 1). Such low pO_2 conditions are also echoed in the numerous indicators of low oxygen in the deep and shallow ocean during this period (Planavsky *et al.,* 2011; Poulton and Canfield, 2011; Reinhard *et al.,* 2013c; Tang *et al.,* 2016). However, a smaller atmospheric O_2 inventory during this period carries with it the potential for somewhat unstable behavior (*e.g.,* Planavsky *et al.,* 2014b), and there is proxy evidence for potential short-term fluctuations in atmospheric pO_2 between $\sim$1.8 and 0.8 Ga (*e.g.,* Sperling *et al.,* 2014; Gilleaudeau *et al.,* 2016).

Geochemical records during the Neoproterozoic ($\sim$1000–541 Ma) suggest significant ocean-atmosphere redox shifts just prior to the Sturtian glacial epoch at *ca.* 720 Ma (Planavsky *et al.,* 2014b; Thomson *et al.,* 2015) followed by a potentially highly dynamic interval leading up to the Precambrian-Cambrian boundary at 541 Ma (Sahoo *et al.,* 2016). Atmospheric pO_2 during the earliest Paleozoic ($\sim$543–400 Ma), though not particularly well constrained at present, was likely higher than that of the late Proterozoic but well below modern (Bergman *et al.,* 2004; Dahl *et al.,* 2010; Lyons *et al.,* 2014). Thereafter, the charcoal record strongly suggests that pO_2 values during most of the last $\sim$400 million years have been above $\sim$50% PAL (*e.g.,* Cope and Chaloner, 1980; Chaloner, 1989), making O_2 a dominant constituent of Earth's atmosphere for most of the last half-billion years (Fig. 1; Table 1).

From a practical perspective, the detection of O_2 can be achieved via proxy by searching for signs of O_3. On the modern Earth, stratospheric O_3 is ultimately derived from the photolysis of atmospheric O_2, which generates oxygen atoms that subsequently combine with O_2 molecules to yield O_3 (the first two of the so-called ''Chapman reactions''):

$$O_2 + h\nu \rightarrow O + O \ (\lambda < 242 \text{ nm})$$

$$O + O_2 + M \rightarrow O_3 + M$$

where M is any inert molecule that can absorb the energy of the excited O_3 molecule following collision between O and O_2 and eventually dissipate it as heat. The column abundance of atmospheric ozone (O_3) shows a nonlinear dependence on the O_2 content of Earth's atmosphere in 1-D photochemical models (Kasting and Donahue, 1980). In addition, both the altitude and overall abundance of peak O_3 increase with ground-level atmospheric pO_2 (Fig. 2A).

Considering this in light of the geochemical records discussed above, it is possible that for much of Earth's history atmospheric O_3 abundance was extremely low. We can estimate the effects of this by using the characteristics of O_3 profiles generated by a suite of 1-D photochemical models (Kasting and Donahue, 1980) to calculate peak O_3 levels in Earth's atmosphere as a function of ground-level pO_2 (Fig. 2B). The results of this exercise suggest that peak mid-Proterozoic atmospheric O_3 would have been $\sim$0.1–1 ppmv based on the ground-level pO_2 values estimated for this time interval (*e.g.,* $pO_2 \sim 0.1$–1% PAL) and many orders of magnitude below this during the Archean. However, during most of the Phanerozoic, and potentially some periods of the Paleoproterozoic, atmospheric O_3 would have been present at values approaching that of the modern Earth (Table 1).

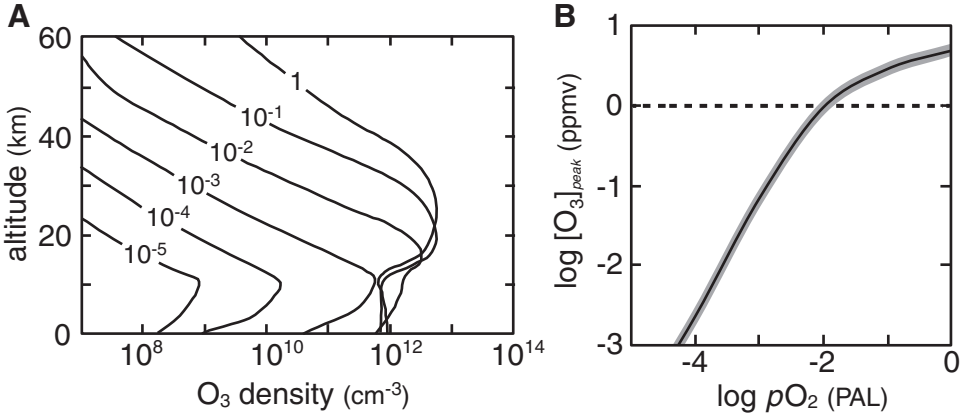

FIG. 2. Shown in (**A**) are number densities for atmospheric ozone (O_3) as a function of altitude calculated from a 1-D photochemical model (after Kasting and Donahue, 1980) at different atmospheric pO_2 values (relative to PAL). The calculations assume a solar zenith angle of 45°. Shown in (**B**) are calculated values of peak atmospheric O_3 as a function of ground-level pO_2 according to the results of Kasting and Donahue (1980). The calculations assume an atmospheric scale height of 7 km and a range of temperatures between 200 and 240 K but are not particularly sensitive to either of these values. The horizontal dashed line denotes a peak O_3 level of 1 ppmv (see text).

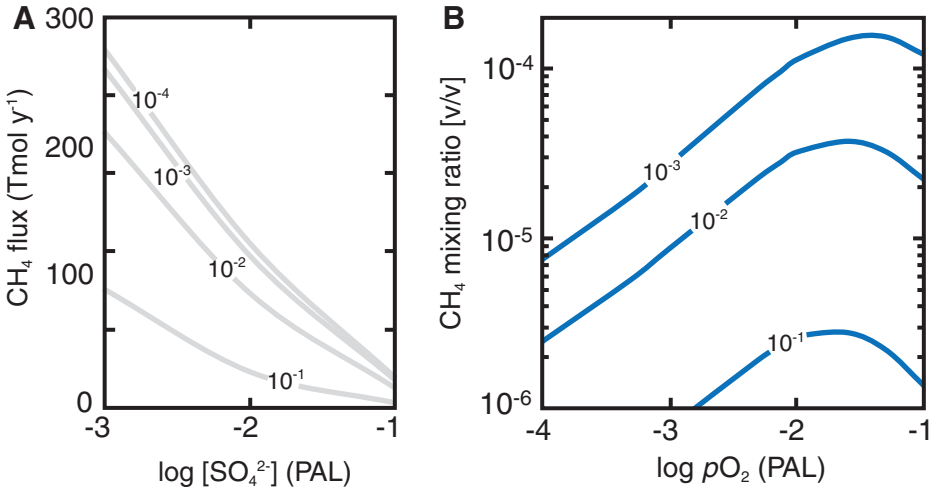

FIG. 3. Representative results from an intermediate-complexity Earth system model of the ocean-atmosphere O_2-O_3-CH_4 cycle. Shown (**A**) are net biospheric CH_4 fluxes to the atmosphere as a function of global average marine sulfate concentration ($[SO_4^{2-}]$), with contours labeled according to atmospheric pO_2 value (relative to PAL). Shown in (**B**) are steady-state atmospheric CH_4 mixing ratios as a function of atmospheric pO_2, with contours labeled according to marine $[SO_4^{2-}]$ (relative to the present oceanic level, POL). Simulations performed under the same default conditions as those in Olson *et al.* (2016).

3. Evolution of Atmospheric CH_4 during Earth's History

Atmospheric O_2/O_3 abundances estimated based on the ground-level pO_2 values discussed above would have had an important impact on another key biosignature gas—methane (CH_4). The relationship between the atmospheric lifetime of CH_4 and the O_2 content of Earth's atmosphere is complex and somewhat counterintuitive. As atmospheric pO_2 drops from 1 to 10^{-1} PAL, the atmospheric lifetime of CH_4 increases as a result of decreasing rates of CH_4 destruction in the atmosphere by hydroxyl radicals (OH). However, once pO_2 drops below $\sim 10^{-2}$ PAL the atmospheric lifetime of CH_4 decreases sharply. This latter behavior arises as a result of increased photochemical production of tropospheric OH as UV shielding by O_3 decreases (Kasting and Donahue, 1980; Pavlov *et al.,* 2000, 2003; Pavlov and Kasting, 2002). An additional complexity is that the atmospheric lifetime of CH_4 is also a highly nonlinear function of its source fluxes from the biosphere and solid Earth (Pavlov *et al.,* 2003), which means that potential oceanic sinks for CH_4 must also be considered in any attempt to diagnose atmospheric pCH_4. Because the biospheric production and consumption fluxes of CH_4 are also directly or indirectly linked to atmospheric O_2 levels via the availability of oxidants at a planet's surface (*e.g.,* O_2, Fe^{3+}, SO_4^{2-}), the quantitative relationship between atmospheric O_2 and CH_4 will be extremely complex on ocean-bearing silicate planets.

Though there is at present no available geochemical proxy for ancient atmospheric CH_4 levels, a number of recent studies have attempted to explicitly model the effect of metabolic CH_4 consumption on surface fluxes and atmospheric pCH_4 (Claire *et al.,* 2006; Catling *et al.,* 2007; Beal *et al.,* 2011; Daines and Lenton, 2016; Olson *et al.,* 2016). The most recent attempt includes both aerobic and anaerobic microbial oxidation of CH_4 within a 3-D model of ocean biogeochemistry coupled to a parameterized O_2-O_3-CH_4 photochemical scheme (Olson *et al.,* 2016). Overall, the results of this work suggest that atmospheric CH_4 levels are extremely sensitive to concentrations of seawater sulfate (SO_4^{2-}). As a result, at atmospheric pO_2 values and marine SO_4^{2-} levels characteristic of the Proterozoic, net biogenic CH_4 fluxes would have been strongly attenuated such that atmospheric pCH_4 was unlikely to have been significantly higher than $\sim$1–10 ppmv (Fig. 3; Olson *et al.,* 2016). However, given recent estimates of Archean seawater SO_4^{2-} levels (Crowe *et al.,* 2014), it is likely that biogenic CH_4 fluxes to the atmosphere would have been much higher during this period. Combined with much lower atmospheric pO_2, these larger fluxes could potentially have led to Archean atmospheric pCH_4 values on the order of $\sim 10^2$ to 10^3 ppmv (Pavlov *et al.,* 2000; Claire *et al.,* 2006; Zahnle *et al.,* 2006; Catling *et al.,* 2007).

4. Remote Detectability of O_2-O_3-CH_4 Biosignatures throughout Earth's History

The actual detectability of any gas in a future exoplanet observation will be a combined function of the abundance of that gas in the atmosphere, the observing parameters (such as distance, stellar host type, background noise, etc.), and the instrumentation with which the observation is made (see, *e.g.,* Robinson *et al.,* 2016). Here, we conduct a qualitative assessment of the potential detectability of O_2, O_3, and CH_4 through geological time by generating synthetic direct-imaging spectra based on scaling a modern midlatitude Earth atmosphere profile (Schwieterman *et al.,* 2015) to the evolving gas abundances throughout Earth's history (Table 1). We use the Spectral Mapping Atmosphere Radiative Transfer Model (SMART; Meadows and Crisp, 1996; Crisp 1997), which is well validated by remote observations of the whole Earth (Robinson *et al.,* 2011, 2014), Venus (Arney *et al.,* 2014), and Mars (Tinetti *et al.,* 2005) and has been previously used in spectral studies of the Archean Earth (Arney *et al.,* 2016). We focus on the O_3 UV Hartley-Huggins bands (centered at $\sim$0.25 μm), the O_2 Fraunhofer

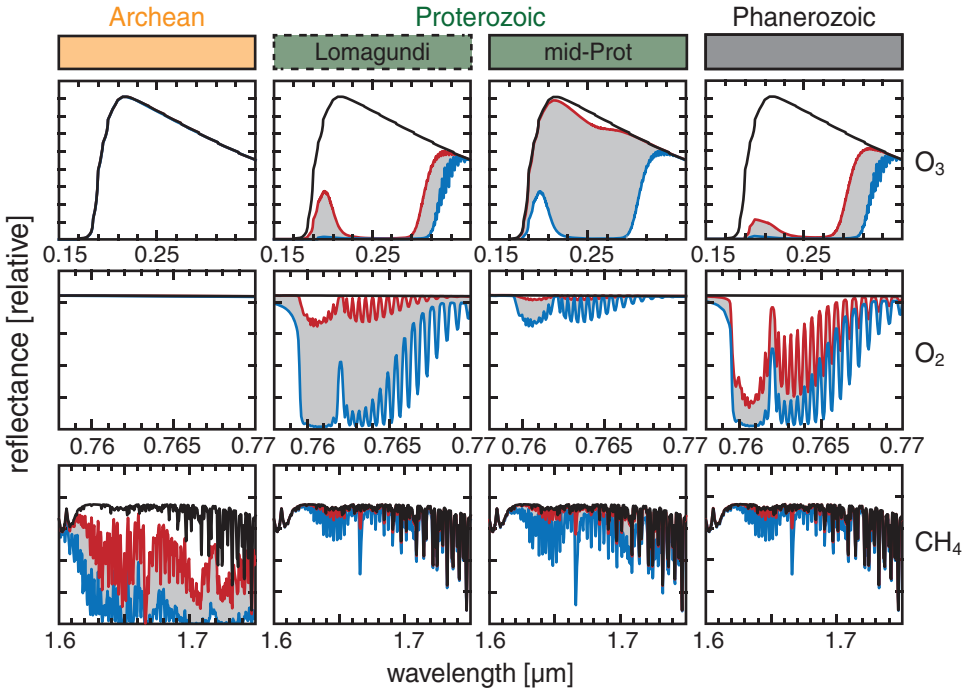

FIG. 4. Reflectance spectra of selected O_2, O_3, and CH_4 bands as a function of geological epoch. Lower abundance limits are given in red, upper limits are given in blue, and the region between these limits is shaded gray. The black line represents the case with no absorption by O_2, O_3, or CH_4. Limits are representative of both uncertainties in atmospheric abundance and variability of those abundances over the course of each epoch (Table 1). Values for peak atmospheric O_3 are calculated as a function of ground-level pO_2 according to the results of Kasting and Donahue (1980). The resolution of each spectrum is 1 cm^{-1}, which is approximately $\Delta\lambda = 6.25 \times 10^{-6}$ μm at 0.25 μm, $\Delta\lambda = 5.78 \times 10^{-5}$ μm at 0.76 μm, and $\Delta\lambda = 2.72 \times 10^{-4}$ μm at 1.65 μm. We used a solar zenith angle of 60° to approximate a disk-average. Note that reflectances are arbitrarily scaled to provide a qualitative assessment of potential detectability.

A band (0.76 μm), and the 1.65 μm CH_4 band as a function of geological epoch (Fig. 4). These bands were chosen in part because they will likely be included in the instrumentation suite of future direct-imaging telescopes (*e.g.,* Dalcanton *et al.,* 2015) and because mid-IR direct imaging of exoplanets is unlikely for the intermediate future.

Molecular oxygen (O_2) has no significant spectral features at mid-IR wavelengths, but it has three significant features in the optical range (Des Marais *et al.,* 2002). These are the so-called ''Fraunhofer'' A and B bands (at 0.76 and 0.69 μm, respectively), along with an additional feature at 1.26 μm. Of these, the Fraunhofer A band is the most prominent but is likely to have appreciable depth only at atmospheric pO_2 levels of ~1% or higher (Fig. 4; Des Marais *et al.,* 2002). Thus, direct detection or quantification of molecular oxygen (O_2) would have been very difficult for much of Earth's history, other than during a transient period of the Paleoproterozoic and during most of the last ~500 million years (Figs. 1 and 4).

Ozone has a number of spectral features in the IR, visible, and UV range, including a strong feature at 9.7 μm, the so-called ''Chappuis'' bands between 0.5 and 0.7 μm, and the ''Hartley-Huggins'' bands at ~0.35–0.2 μm (Des Marais *et al.,* 2002; Domagal-Goldman *et al.,* 2014). The most promising of these from a detection standpoint is the combined Hartley-Huggins band in the near-UV centered at ~0.25 μm (Fig. 4), which is the most sensitive to small O_2 abundance and saturates at O_3 fractions of <1 ppmv. This band is also important because it lies within the proposed instrument range for space-based telescope missions currently under consideration (Dalcanton *et al.,* 2015; Mennesson *et al.,* 2016).

Peak O_3 abundances near the upper range of Proterozoic estimates would potentially have been a promising candidate for detection via the UV-Hartley band, but even this feature may have been challenging to observe at the lower end of pO_2 estimates. Combined with atmospheric pO_2 values orders of magnitude below this during the Archean, atmospheric O_2 (and possibly O_3) would perhaps have been difficult to detect remotely in Earth's atmosphere for most of its history. A potential exception to this early signal gap exists in the ''O_2 overshoot'' hypothesized for the Paleoproterozoic (see above), representing the fascinating possibility of a transiently detectable O_2-rich biogenic atmosphere during Earth's early history followed by over a billion years of predominantly undetectable O_2/O_3 levels. Possible shifts to more elevated pO_2 on shorter timescales between ~1.8 and 0.8 Ga (*e.g.,* Planavsky *et al.,* 2014b; Sperling *et al.,* 2014; Gilleaudeau *et al.,* 2016) should also be explored for their plausibility as biosignature windows.

Methane has a number of features in the mid-IR and visible to near-IR ranges, including five weak features between 0.6 and 1.0 μm, two at 1.65 and 2.4 μm, and a significant feature at ~7.7–8.2 μm. The 1.65 μm CH_4 band would likely have been visible during Archean time (Fig. 4), but the 0.6–1.0 μm features are only expected to have appreciable depth at pCH_4

above $\sim 10^3$ ppmv (Des Marais *et al.,* 2002). In any case, in light of the model results discussed above it is possible that atmospheric CH_4 would have been a challenging detection for the last ~ 2.5 billion years of Earth's history (*e.g.,* subsequent to the GOE), at least via low- to moderate-resolution spectroscopy. However, the very low atmospheric pO_2 and oceanic SO_4^{2-} concentrations reconstructed for Archean time leave open the possibility that CH_4 would have been remotely detectable in Earth's atmosphere for the better part of Earth's first ~ 2 billion years (Fig. 4).

5. Discussion and Conclusions

By combining the geochemical reconstructions, Earth-system model results, and spectral considerations discussed above, we can place the O_2-O_3-CH_4 disequilibrium biosignature on Earth in a broader temporal context as a possible analogue for terrestrial exoplanets. Currently available proxy and model constraints indicate that, during the Archean (~ 3.8–2.5 Ga), atmospheric CH_4 levels may have been generally within or above the range that would be remotely detectable. In contrast, atmospheric O_2 levels were many orders of magnitude below detection of either O_2 or O_3, with the possible exception of pulsed pO_2 increases during the late Archean (*e.g.,* Anbar *et al.,* 2007; Kendall *et al.,* 2015). Combined proxy and model results indicate that, during the mid-Proterozoic, both O_2 and CH_4 would have been undetectable and are consistent with the possibility that O_3 would have been challenging to detect. An interesting exception to this may have occurred during the Paleoproterozoic, between ~ 2.2 and 2.0 Ga, when atmospheric pO_2 may have been elevated to detectable levels before decreasing again for over a billion years. Following possibly dynamic upheavals in ocean-atmosphere redox during the late Proterozoic, atmospheric O_2/O_3 was present at levels that would likely have been readily detectable for most of the last ~ 500 million years. However, results from Earth system models indicate that detection of atmospheric CH_4 would have been problematic with low- to moderate-resolution spectroscopy during this same period.

The realization that Earth's biosphere may have remained cryptic to conventional methods of remote detection for large periods of its history highlights the need to explore novel atmospheric biosignatures (Pilcher, 2003; Domagal-Goldman *et al.,* 2011; Seager *et al.,* 2013a) and provides further impetus for wide-ranging and systematic exploration of possible atmospheric biosignatures for application in a range of scenarios. Our results also highlight the importance of developing contextual plausibility arguments for biogenic gases in reducing atmospheres and, in particular, the presence/absence and characteristics of exoplanetary oceans. In this light, observations of time-resolved changes in atmospheric chemistry (*e.g.,* seasonality) that can be firmly linked to quantitative models for biotic and abiotic sources will be important to consider. For example, although there may be plausible abiotic routes to high CH_4 in a reducing planetary atmosphere, it may be much more difficult to generate seasonal variations in atmospheric pCH_4 without an active surface biosphere.

Our analysis suggests that a planet with a biosphere largely (or entirely) confined to the marine realm will in many cases remain invisible to remote detection as a result of biosignature filtering by ocean biogeochemistry—a difficulty that may apply to both presence/absence and thermodynamic techniques. Our analysis suggests that the possible detection of oceans at a planet's surface (Robinson *et al.,* 2010; but see Cowan *et al.,* 2012) is a critical piece of contextual information for validating potential atmospheric biosignatures, and that planets with terrestrial biospheres (*e.g.,* partially or entirely subaerial in scope) may be the most readily detected and characterized because of their more direct geochemical exchange with the overlying atmosphere. Ironically, in some cases planets that are very conducive to the development and maintenance of a pervasive biosphere, with large inventories of H_2O and extensive oceans, may at times be the most difficult to characterize via conventional biosignature techniques.

Although our results are broadly applicable to Earth-analog planets orbiting Sun-like stars, additional work will be necessary to determine the extent to which differences in the stellar environment may impact the buildup of O_2 and CH_4 (*e.g.,* Loyd *et al.,* 2016; Meadows *et al.,* 2016), while also considering the effects of ocean chemistry, as we have done here. Nevertheless, our work further stresses the importance of including and refining UV observations for exploration of potentially habitable exoplanets, since it is quite plausible that Proterozoic Earth analogues would have detectable O_3 without spectrally apparent O_2. Moreover, high-resolution spectroscopy ($R > 20{,}000$), coupled with high-contrast imaging, may provide a promising avenue for detecting modern Earth-like CH_4 abundances on an exoplanet (*e.g.,* Snellen *et al.,* 2015), though the feasibility of this technique has yet to be conclusively demonstrated. We would recommend investigation of this technique as perhaps the only plausible approach toward observing the O_2-CH_4 biosignature couple in true Earth analogues. More broadly, our analysis highlights the importance of including a rigorous understanding of ocean biogeochemistry into models of biosignature production and preservation on exoplanets and affirms that critical insights into the evolution of atmospheric biosignatures on Earth-like planets can be provided by better understanding Earth's dynamic history.

Acknowledgments

C.T.R. and T.W.L. acknowledge support from the NASA Astrobiology Institute. C.T.R. acknowledges support from the Alfred P. Sloan Foundation. E.W.S. acknowledges support from the NASA Astrobiology Institute Director's Discretionary Fund and the NASA Postdoctoral Program, administered by the Universities Space Research Association. This work benefited from the use of advanced computational, storage, and networking infrastructure provided by the Hyak supercomputer system at the University of Washington.

References

Akeson, R.L., Chen, X., Ciardi, D., Crane, M., Good, J., Harbut, M., Jackson, E., Kane, S.R., Laity, A.C., Leifer, S., Lynn, M., McElroy, D.L., Papin, M., Plavchan, P., Ramírez, S.V., Rey, R., von Braun, K., Wittman, M., Abajian, M., Ali, B., Beichman, C., Beekley, A., Berriman, G.B., Berukoff, S., Bryden, G., Chan, B., Groom, S., Lau, C., Payne, A.N., Regelson, M., Saucedo, M., Schmitz, M., Stauffer, J., Wyatt, P.,

and Zhang, A. (2013) The NASA Exoplanet Archive: data and tools for exoplanet research. *Publ Astron Soc Pac* 125: 989–999.

Anbar, A.D., Duan, Y., Lyons, T.W., Arnold, G.L., Kendall, B., Creaser, R.A., Kaufman, A.J., Gordon, G.W., Scott, C., Garvin, J., and Buick, R. (2007) A whiff of oxygen before the Great Oxidation Event? *Nature* 317:1903–1906.

Arney, G., Meadows, V., Crisp, D., Schmidt, S.J., Bailey, J., and Robinson, T. (2014) Spatially resolved measurements of H_2O, HCl, CO, OCS, SO_2, cloud opacity, and acid concentration in the Venus near-infrared spectral windows. *J Geophys Res: Planets* 119:1860–1891.

Arney, G., Domagal-Goldman, S.D., Meadows, V.S., Wolf, E.T., Schwieterman, E., Charnay, B., Claire, M., Hébrard, E., and Trainer, M.G. (2016) The pale orange dot: the spectrum and habitability of hazy Archean Earth. *Astrobiology* 16:873–899.

Bartdorff, O., Wallmann, K., Latif, M., and Semenov, V. (2008) Phanerozoic evolution of atmospheric methane. *Global Biogeochem Cycles* 22, doi:10.1029/2007GB002985.

Beal, E.J., Claire, M.W., and House, C.H. (2011) High rates of anaerobic methanotrophy at low sulfate concentrations with implications for past and present methane levels. *Geobiology* 9:131–139.

Bergman, N.M., Lenton, T.M., and Watson, A.J. (2004) COPSE: a new model of biogeochemical cycling over Phanerozoic time. *Am J Sci* 304:397–437.

Canfield, D.E., Ngombi-Pemba, L., Hammarlund, E.U., Bengston, S., Chaussidon, M., Gauthier-Lafaye, F., Meunier, A., Riboulleau, A., Rollion-Bard, C., Rouxel, O., Asael, D., Pierson-Wickmann, A., and El Albani, A. (2015) Oxygen dynamics in the aftermath of the Great Oxidation of Earth's atmosphere. *Proc Natl Acad Sci USA* 110:16736–16741.

Catling, D.C. and Claire, M.W. (2005) How Earth's atmosphere evolved to an oxic state: a status report. *Earth Planet Sci Lett* 237:1–20.

Catling, D.C., Claire, M.W., and Zahnle, K.J. (2007) Anaerobic methanotrophy and the rise of atmospheric oxygen. *Philos Transact A Math Phys Eng Sci* 365:1867–1888.

Chaloner, W.G. (1989) Fossil charcoal as an indicator of paleoatmospheric oxygen level. *J Geol Soc London* 146:171–174.

Claire, M.W., Catling, D.C., and Zahnle, K.J. (2006) Biogeochemical modelling of the rise in atmospheric oxygen. *Geobiology* 4:239–269.

Cole, D.B., Reinhard, C.T., Wang, X., Bueguen, B., Halverson, G.P., Lyons, T.W., and Planavsky, N.J. (2016) A shale-hosted Cr isotope record of low atmospheric oxygen during the Proterozoic. *Geology* 44:555–558.

Cope, M.J. and Chaloner, W.G. (1980) Fossil charcoal as evidence of past atmospheric composition. *Nature* 283:647–649.

Cowan, N.B., Abbot, D.S., and Voigt, A. (2012) A false positive for ocean glint on exoplanets: the latitude-albedo effect. *Astrophys J* 752:L3–L7.

Cowan, N.B., Greene, T., Angerhausen, D., Batalha, N.E., Clampin, M., Colón, K., Crossfield, I.J.M., Fortney, J.J., Gaudi, B.S., Harrington, J., Iro, N., Lillie, C.F., Linsky, J.L., Lopez-Morales, M., Mandell, A.M., and Stevenson, K.B. (2015) Characterizing transiting planet atmospheres through 2025. *Publ Astron Soc Pac* 127:311–327.

Crisp, D. (1997) Absorption of sunlight by water vapor in cloudy conditions: a partial explanation for the cloud absorption anomaly. *Geophys Res Lett* 24:571–574.

Crowe, S.A., Døssing, L.N., Beukes, N.J., Bau, M., Kruger, S.J., Frei, R., and Canfield, D.E. (2013) Atmospheric oxygenation three billion years ago. *Nature* 501:535–538.

Crowe, S.A., Paris, G., Katsev, S., Jones, C., Kim, S.-T., Zerkle, A.L., Nomosatryo, S., Fowle, D.A., Adkins, J.F., Sessions, A.L., Farquhar, J., and Canfield, D.E. (2014) Sulfate was a trace constituent of Archean seawater. *Science* 346: 735–739.

Dahl, T.W., Hammarlund, E.U., Anbar, A.D., Bond, D.P.G., Gill, B.C., Gordon, G.W., Knoll, A.H., Nielsen, A.T., Schovsbo, N.H., and Canfield, D.E. (2010) Devonian rise in atmospheric oxygen correlated to the radiations of terrestrial planets and large predatory fish. *Proc Natl Acad Sci USA* 107:17911–17915.

Daines, S.J. and Lenton, T.M. (2016) The effect of widespread early aerobic marine ecosystems on methane cycling and the Great Oxidation. *Earth Planet Sci Lett* 434:42–51.

Dalcanton, J., Seager, S., Aigrain, S., Hirata, C., Battel, S., Mather, J., Brandt, N., Postman, M., Conroy, C., Redding, D., Feinberg, L., Schiminiovich, D., Gezari, S., Stahl, H.P., Guyon, O., Tumilinson, J., and Harris, W. (2015) *From Cosmic Birth to Living Earths: A Visionary Space Telescope for UV-Optical-NearIR Astronomy,* Association of Universities for Research in Astronomy, Washington, DC. Available online at http://www.hdstvision.org/report

Deming, D., Seager, S., Winn, J., Miller-Ricci, E., Clampin, M., Lindler, D., Greene, T., Charbonneau, D., Laughlin, G., Ricker, G., Latham, D., and Enninco, K. (2009) Discovery and characterization of transiting super Earths using an all-sky transit survey and follow-up by the James Webb Space Telescope. *Publ Astron Soc Pac* 121:952–967.

Des Marais, D.J., Harwit, M.O., Jucks, K.W., Kasting, J.F., Lin, D.N., Lunine, J.I., Schneider, J., Seager, S., Traub, W.A., and Woolf, N.J. (2002) Remote sensing of planetary properties and biosignatures on extrasolar terrestrial planets. *Astrobiology* 2:153–181.

Deutzmann, J.S., Stief, P., Brandes, J.A., and Schink, B. (2014) Anaerobic methane oxidation coupled to denitrification is the dominant methane sink in a deep lake. *Proc Natl Acad Sci USA* 111:18273–18278.

Domagal-Goldman, S.D., Meadows, V.S., Claire, M.W., and Kasting, J.F. (2011) Using biogenic sulfur gases as remotely detectable biosignatures on anoxic planets. *Astrobiology* 11: 419–441.

Domagal-Goldman, S.D., Segura, A., Claire, M.W., Robinson, T.D., and Meadows, V.S. (2014) Abiotic ozone and oxygen in atmospheres similar to prebiotic Earth. *Astrophys J* 792, doi:10.1088/0004-637X/792/2/90.

Farquhar, J., Bao, H., and Thiemens, M. (2000) Atmospheric influence of Earth's earliest sulfur cycle. *Science* 289:756–758.

Farquhar, J., Savarino, J., Airieau, S., and Thiemens, M. (2001) Observation of wavelength-sensitive mass-independent sulfur isotope effects during SO_2 photolysis: implications for the early atmosphere. *J Geophys Res* 106:1–11.

Gao, P., Hu, R., Robinson, T.D., Li, C., and Yung, Y.L. (2015) Stability of CO_2 atmospheres on desiccated M dwarf exoplanets. *Astrophys J* 806, doi:10.1088/0004-637X/806/2/249.

Gardner, J.P., Mather, J.C., Clampin, M., Doyon, R., Greenhouse, M.A., Hammel, H.B., Hutchings, J.B., Jakobsen, P., Lilly, S.J., Long, K.S., Lunine, J.I., McCaughrean, M.J., Mountain, M., Nella, J., Rieke, G.H., Rieke, M.J., Rix, H., Smith, E.P., Sonneborn, G., Stiavelli, M., Stockman, H.S.,

Windhorst, R.A., and Wright, G.S. (2006) The James Webb Space Telescope. *Space Sci Rev* 123:485–606.

Gilleaudeau, G.J., Frei, R., Kaufman, A.J., Kah, L.C., Azmy, K., Bartley, J.K., Chernyavskiy, P., and Knoll, A.H. (2016) Oxygenation of the mid-Proterozoic atmosphere: clues from chromium isotopes in carbonates. *Geochemical Perspectives Letters* 2:178–187.

Glasspool, I.J. and Scott, A.C. (2010) Phanerozoic concentrations of atmospheric oxygen reconstructed from sedimentary charcoal. *Nat Geosci* 3:627–630.

Harman, C.E., Schwieterman, E.W., Schottelkotte, J.C., and Kasting, J.F. (2015) Abiotic O_2 levels on planets around F, G, K, and M stars: possible false positives for life? *Astrophys J* 812, doi:10.1088/0004-637X/812/2/137.

Hitchcock, D.R. and Lovelock, J.E. (1967) Life detection by atmospheric analysis. *Icarus* 7:149–159.

Hoehler, T.M., Alperin, M.J., Albert, D.B., and Martens, C.S. (1994) Field and laboratory studies of methane oxidation in an anoxic marine sediment: evidence for a methanogen-sulfate reducer consortium. *Global Biogeochem Cycles* 8: 451–463.

Holland, H.D. (1984) *The Chemical Evolution of the Atmosphere and Ocean,* Princeton University Press, Princeton, NJ.

Holland, H.D. (2002) Volcanic gases, black smokers, and the Great Oxidation Event. *Geochim Cosmochim Acta* 66:3811–3826.

Johnston, D.T. (2011) Multiple sulfur isotopes and the evolution of Earth's surface sulfur cycle. *Earth-Science Reviews* 106: 161–183.

Kaltenegger, L., Traub, W.A., and Jucks, K.W. (2007) Spectral evolution of an Earth-like planet. *Astrophys J* 658:598–616.

Kasting, J.F. (1991) Box models for the evolution of atmospheric oxygen. *Glob Planet Change* 97:125–131.

Kasting, J.F. and Donahue, T.M. (1980) The evolution of atmospheric ozone. *J Geophys Res: Oceans and Atmospheres* 85:3255–3263.

Kendall, B., Creaser, R.A., Reinhard, C.T., Lyons, T.W., and Anbar, A.D. (2015) Transient episodes of mild environmental oxygenation and oxidative continental weathering during the late Archean. *Sci Adv* 1, doi:10.1126/sciadv.1500777.

Krissanson-Totton, J., Bergsman, D.S., and Catling, D.C. (2016) On detecting biospheres from chemical thermodynamic disequilibrium in planetary atmospheres. *Astrobiology* 16:39–67.

Lovelock, J.E. (1965) A physical basis for life detection experiments. *Nature* 207:568–570.

Loyd, R.O.P., France, K., Youngblood, A., Schneider, C., Brown, A., Hu, R., Linsky, J., Froning, C.S., Redfield, S., Rugheimer, S., and Tian, F. (2016) The MUSCLES Treasury Survey. III. X-ray to infrared spectra of 11 M and K stars hosting planets. *Astrophys J* 824, doi:10.3847/0004-637X/824/2/102.

Luger, R. and Barnes, R. (2015) Extreme water loss and abiotic O_2 buildup on planets throughout the habitable zones of M dwarfs. *Astrobiology* 15:119–143.

Luo, G., Ono, S., Beukes, N.J., Wang, D.T., Xie, S., and Summons, R.E. (2016) Rapid oxygenation of Earth's atmosphere 2.33 billion years ago. *Sci Adv* 2, doi:10.1126/sciadv.1600134.

Lyons, T.W., Reinhard, C.T., and Planavsky, N.J. (2014) The rise of oxygen in Earth's early ocean and atmosphere. *Nature* 506:307–315.

Martens, C.S. and Berner, R.A. (1977) Interstitial water chemistry of anoxic Long Island Sound sediments. 1. Dissolved gases. *Limnol Oceanogr* 22:10–25.

Mayor, M. and Queloz, D. (1995) A Jupiter-mass companion to a solar-type star. *Nature* 378:355–359.

Meadows, V.S. and Crisp, D. (1996) Ground-based near-infrared observations of the Venus nightside: the thermal structure and water abundance near the surface. *J Geophys Res* 101:4595–4622.

Meadows, V.S. and Seager, S. (2010) Terrestrial planet atmospheres and biosignatures. In *Exoplanets,* edited by S. Seager, University of Arizona Press, Tucson, AZ, pp 441–470.

Meadows, V.S., Arney, G.N., Schwieterman, E.W., Lustig-Yaeger, J., Lincowski, A.P., Robinson, T., Domagal-Goldman, S.D., Barnes, R.K., Fleming, D.P., Deitrick, R., Luger, R., Driscoll, P.E., Quinn, T.R., and Crisp, D. (2016) The habitability of Proxima Centauri b: II: environmental states and observational discriminants. arXiv: 1608.08620

Mennesson, B., Gaudi, S., Seager, S., Cahoy, K., Domagal-Goldman, S., Feinberg, L., Guyon, O., Kasdin, J., Marois, C., Mawet, D., Tamura, M., Mouillet, D., Prusti, T., Quirrenbach, A., Robinson, T., Rogers, L., Scowen, P., Somerville, R., Stapelfeldt, K., Stern, D., Still, M., Turnbull, M., Booth, J., Kiessling, A., Kuan, G., and Warfield, K. (2016) The Habitable Exoplanet (HabEx) Imaging Mission: preliminary science drivers and technical requirements. *Proc SPIE* 9904, doi:10.1117/12.2240457.

Olson, S.L., Kump, L.R., and Kasting, J.F. (2013) Quantifying the areal extent and dissolved oxygen concentrations of Archean oxygen oases. *Chem Geol* 362:35–43.

Olson, S.L., Reinhard, C.T., and Lyons, T.W. (2016) Limited role for methane in the mid-Proterozoic greenhouse. *Proc Natl Acad Sci USA* 113:11447–11452.

Ono, S., Eigenbrode, J.L., Pavlov, A.A., Kharecha, P., Rumble, D., III, Kasting, J.F., and Freeman, K.H. (2003) New insights into Archean sulfur cycle from mass-independent sulfur isotope records from the Hamersley Basin, Australia. *Earth Planet Sci Lett* 213:15–30.

Partin, C.A., Bekker A., Planavsky, N.J., Scott, C.T., Gill, B.C., Li, C., Podkovyrov, V., Maslov, A., Konhauser, K.O., Lalonde, S.V., Love, G.D., Poulton, S.W., and Lyons, T.W. (2013) Large-scale fluctuations in Precambrian atmospheric and oceanic oxygen levels from the record of U in shales. *Earth Planet Sci Lett* 369–370:284–293.

Pavlov, A.A. and Kasting, J.F. (2002) Mass-independent fractionation of sulfur isotopes in Archean sediments: strong evidence for an anoxic Archean atmosphere. *Astrobiology* 2:27–41.

Pavlov, A.A., Kasting, J.F., and Brown, L.L. (2000) Greenhouse warming by CH_4 in the atmosphere of early Earth. *J Geophys Res* 105:11981–11990.

Pavlov, A.A., Hurtgen, M.T., Kasting, J.F., and Arthur, M.A. (2003) Methane-rich Proterozoic atmosphere? *Geology* 31: 87–90.

Pierrehumbert, R.T. (2013) Strange news from other stars. *Nat Geosci* 6:81–83.

Pilcher, C.B. (2003) Biosignatures of early Earths. *Astrobiology* 3:471–486.

Planavsky, N.J., McGoldrick, P., Scott, C.T., Li, C., Reinhard, C.T., Kelly, A.E., Chu, X.L., Bekker, A., Love, G.D., and

Lyons, T.W. (2011) Widespread iron-rich conditions in the mid-Proterozoic ocean. *Nature* 477:448–451.

Planavsky, N.J., Bekker, A., Hofmann, A., Owens, J.D., and Lyons, T.W. (2012) Sulfur record of rising and falling marine oxygen and sulfate levels during the Lomagundi event. *Proc Natl Acad Sci USA* 109:18300–18305.

Planavsky, N.J., Asael, D., Hofmann, A., Reinhard, C.T., Lalonde, S.V., Knudsen, A., Wang, X., Ossa Ossa, F., Pecoits, E., Smith, A.J.B., Beukes, N.J., Bekker, A., Johnson, T.M., Konhauser, K.O., Lyons, T.W., and Rouxel, O.J. (2014a) Evidence for oxygenic photosynthesis half a billion years before the Great Oxidation Event. *Nat Geosci* 7:283–286.

Planavsky, N.J., Reinhard, C.T., Wang, X., Thomson, D., McGoldrick, P., Rainbird, R.H., Johnson, T.M., Fischer, W.W., and Lyons, T.W. (2014b) Low mid-Proterozoic atmospheric oxygen levels and the delayed rise of animals. *Science* 346:635–638.

Poulton, S.W. and Canfield D.E. (2011) Ferruginous conditions: a dominant feature of the ocean through Earth's history. *Elements* 7:107–112.

Reeburgh, W.S. (2007) Oceanic methane biogeochemistry. *Chem Rev* 107:486–513.

Regnier, P., Dale, A.W., Arndt, S., LaRowe, D.E., Mogollón, J., and Van Cappellen, P. (2011) Quantitative analysis of anaerobic oxidation of methane (AOM) in marine sediments: a modeling perspective. *Earth-Science Reviews* 106:105–130.

Reinhard, C.T., Raiswell, R., Scott, C., Anbar, A.D., and Lyons, T.W. (2009) A Late Archean sulfidic sea stimulated by early oxidative weathering of the continents. *Science* 326:713–716.

Reinhard, C.T., Lalonde, S., and Lyons, T.W. (2013a) Oxidative sulfide dissolution on the early Earth. *Chem Geol* 362: 44–55.

Reinhard, C.T., Planavsky, N.J., and Lyons, T.W. (2013b) Long-term sedimentary recycling of rare sulphur isotope anomalies. *Nature* 297:100–103.

Reinhard, C.T., Planavsky, N.J., Robbins, L.J., Partin, C.A., Gill, B.C., Lalonde, S.V., Bekker, A., Konhauser, K.O., and Lyons, T.W. (2013c) Proterozoic ocean redox and biogeochemical stasis. *Proc Natl Acad Sci USA* 110:5357–5362.

Reinhard, C.T., Planavsky, N.J., Olson, S.L., Lyons, T.W., and Erwin, D.H. (2016) Earth's oxygen cycle and the evolution of animal life. *Proc Natl Acad Sci USA* 113:8933–8938.

Riedinger, N., Formolo, M.J., Lyons, T.W., Henkel, S., Beck, A., and Kasten, S. (2014) An inorganic geochemical argument for coupled anaerobic oxidation of methane and iron reduction in marine sediments. *Geobiology* 12:172–181.

Robinson, T.D., Meadows, V.S., and Crisp, D. (2010) Detecting oceans on extrasolar planets using the glint effect. *Astrophys J* 721:L67–L71.

Robinson, T.D., Meadows, V.S., Crisp, D., Deming, D., A'Hearn, M.F., Charbonneau, D., Livengood, T.A., Seager, S., Barry, R.K., Hearty, T., Hewagama, T., Lisse, C.M., McFadden, L., and Wellnitz, D.D. (2011) Earth as an extrasolar planet: Earth model validation using EPOXI Earth observations. *Astrobiology* 11:393–408.

Robinson, T.D., Ennico, K., Meadows, V.S., Sparks, W., Bussey, D.B.J., Schwieterman, E.W., and Breiner, J. (2014) Detection of ocean glint and ozone absorption using LCROSS Earth observations. *Astrophys J* 787, doi:10.1088/0004-637X/787/2/171.

Robinson, T.D., Stapelfeldt, K.R., and Marley, M.S. (2016) Characterizing rocky and gaseous exoplanets with 2 m class space-based coronagraphs. *Publ Astron Soc Pac* 128, doi:10.1088/1538-3873/128/960/025003.

Rye, R. and Holland, H.D. (1998) Paleosols and the evolution of atmospheric oxygen: a critical review. *Am J Sci* 298:621–672.

Sagan, C., Thompson, W.R., Carlson, R., Gurnett, D., and Hord, C. (1993) A search for life on Earth from the Galileo spacecraft. *Nature* 365:715–721.

Sahoo, S.K., Planavsky, N.J., Jiang, G., Kendall, B., Owens, J.D., Wang, X., Shi, X., Anbar, A.D., and Lyons, T.W. (2016) Oceanic oxygenation events in the anoxic Ediacaran ocean. *Geobiology* 14:457–468.

Schröder, S., Bekker, A., Beukes, N.J., Strauss, H., and van Niekerk, H.S. (2008) Rise in seawater sulphate concentration associated with the Paleoproterozoic positive carbon isotope excursion: evidence from sulphate evaporites in the ~2.2–2.1 Gyr shallow-marine Lucknow Formation, South Africa. *Terra Nova* 20:108–117.

Schwieterman, E.W., Robinson, T.D., Meadows, V.S., Misra, A., and Domagal-Goldman, S. (2015) Detecting and constraining N_2 abundances in planetary atmospheres using collisional pairs. *Astrophys J* 810, doi:10.1088/0004-637X/810/1/57.

Schwieterman, E.W., Meadows, V.S., Domagal-Goldman, S.D., Deming, D., Arney, G.N., Luger, R., Harman, C.E., Misra, A., and Barnes, R. (2016) Identifying planetary biosignature impostors: spectral features of CO and O_4 resulting from abiotic O_2/O_3 production. *Astrophys J* 819:L13.

Seager, S. (2013) Exoplanet habitability. *Science* 340:577–581.

Seager, S. (2014) The future of spectroscopic life detection on exoplanets. *Proc Natl Acad Sci USA* 111:12634–12640.

Seager, S. and Deming, D. (2011) Exoplanet atmospheres. *Annu Rev Astron Astrophys* 48:631–672.

Seager, S., Bains, W., and Hu, R. (2013a) A biomass-based model to estimate the plausibility of exoplanet biosignature gases. *Astrophys J* 775, doi:10.1088/0004-637X/775/2/104.

Seager, S., Bains W., and Hu, R. (2013b) Biosignature gases in H_2-dominated atmospheres on rocky exoplanets. *Astrophys J* 777, doi:10.1088/0004-637X/777/2/95.

Segura, A., Meadows, V.S., Kasting, J.F., Crisp, D., and Cohen, M. (2007) Abiotic formation of O_2 and O_3 in high-CO_2 terrestrial atmospheres. *Astron Astrophys* 472:665–679.

Sivan, O., Adler, M., Pearson, A., Gelman, F., Bar-Or, I., John, S.G., and Eckert, W. (2011) Geochemical evidence for iron-mediated anaerobic oxidation of methane. *Limnol Oceanogr* 56:1536–1544.

Snellen, I.A.G., de Kok, R.J., le Poole, R., Brogi, M., and Birkby, J. (2013) Finding extraterrestrial life using ground-based high-dispersion spectroscopy. *Astrophys J* 764, doi: 10.1088/0004-637X/764/2/182.

Snellen, I.A.G., de Kok, R.J., Birkby, J.L., Brandl, B., Brogi, M., Keller, C.U., Kenworthy, M., Schwarz, H., and Stuik, R. (2015) Combining high-dispersion spectroscopy with high contrast imaging: probing rocky planets around our nearest neighbors. *Astron Astrophys* 576:A59.

Sperling, E.A., Rooney, A.D., Hays, L.E., Sergeev, V.N., Vorob'eva, N.G., Sergeeva, N.D., Selby, D., Johnston, D.T., and Knoll, A.H. (2014) Redox heterogeneity of subsurface waters in the Mesoproterozoic ocean. *Geobiology* 12:373–386.

Tang, D., Shi, X., Wang, X., and Jiang, G. (2016) Extremely low oxygen concentration in mid-Proterozoic shallow seawaters. *Precambrian Res* 276:145–157.

Thomson, D., Rainbird, R.H., Planavsky, N., Lyons, T.W., and Bekker, A. (2015) Chemostratigraphy of the Shaler Supergroup, Victoria Island, NS Canada: a record of ocean com-

position prior to the Cryogenian glaciations. *Precambrian Res* 263:232–245.

Tinetti, G., Meadows, V.S., Crisp, D., Fong, W., Velusamy, T., and Snively, H. (2005) Disk-averaged synthetic spectra of Mars. *Astrobiology* 5:461–482.

Ueno, Y., Johnson, M.S., Danielache, S.O., Eskebjerg, C., Pandey, A., and Yoshida, N. (2009) Geological sulfur isotopes indicate elevated OCS in the Archean atmosphere, solving faint young Sun paradox. *Proc Natl Acad Sci USA* 106:14784–14789.

Valentine, D.L. (2011) Emerging topics in marine methane biogeochemistry. *Ann Rev Mar Sci* 3:147–171.

Wordsworth, R. and Pierrehumbert R.T. (2014) Abiotic oxygen-dominated atmospheres on terrestrial habitable zone planets. *Astrophys J* 785:L20.

Zahnle, K.J., Claire, M., and Catling, D. (2006) The loss of mass-independent fractionation in sulfur due to a Paleoproterozoic collapse of atmospheric methane. *Geobiology* 4:271–283.

Address correspondence to:
Christopher T. Reinhard
School of Earth and Atmospheric Sciences
Georgia Institute of Technology
311 Ferst Dr.
Atlanta, GA 30332

E-mail: chris.reinhard@eas.gatech.edu

Submitted 28 September 2016
Accepted 23 January 2017

Abbreviations Used

GOE = Great Oxidation Event
PAL = present atmospheric level